Pressure-driven mechanical anisotropy and destabilization in zeolitic imidazolate frameworks

Pressure Driven Mechanical Anisotropy and Destabilization in Zeolitic Imidazolate Frameworks

Jefferson Maul,[1] Matthew R. Ryder,[2] Michael T. Ruggiero,[3] and Alessandro Erba[1,*]

[1] *Dipartimento di Chimica, Universitá di Torino, via Giuria 5, 10125, Torino, Italy*
[2] *Neutron Scattering Division, Oak Ridge National Laboratory, Oak Ridge, Tennessee 37831, United States of America*
[3] *Department of Chemistry, University of Vermont, 82 University Place, Burlington, VT, 05405, United States of America*

(Dated: October 17, 2018)

The anisotropic mechanical response of ZIF-8 and ZIF-67 is investigated as a function of pressure and its main features (including shear-destabilization eventually leading to amorphization) discussed in terms of specific lattice vibrations and structural changes occurring in the framework. At zero pressure, the two ZIFs are characterized by an elastic anisotropy with directions of maximum and minimum stiffness along $\langle 111 \rangle$ and $\langle 100 \rangle$, respectively. At $P = 0.2$ GPa, the framework exhibits a perfectly isotropic mechanical response while at $P > 0.2$ GPa a different (complementary) anisotropic response is observed with directions of maximum and minimum stiffness along $\langle 100 \rangle$ and $\langle 111 \rangle$, respectively. The bulk modulus of the two ZIFs initially slightly increases up to 0.1 GPa of pressure and then decreases at higher pressures. Amorphization in both ZIF-8 and ZIF-67 is confirmed to be due to the pressure-driven mechanical instability of their frameworks to shear deformations. The directional elastic moduli of the two ZIFs are partitioned into contributions from specific normal modes of vibration. The elastic constants C_{11}, and C_{12} (and thus the bulk modulus $K = 1/3(C_{11} + 2C_{12})$) are mostly affected by symmetric "gate-opening" vibrations of the imidazolate linkers in the four-membered rings. The C_{44} shear elastic constant (and thus the mechanical instability and amorphization of the framework) are instead related to asymmetric "gate-opening" vibrations of the four-membered rings.

I. INTRODUCTION

Over the past few years, metal-organic frameworks (MOFs) have been recognized for their unique mechanochemical properties that have made them potential candidates in a variety of applications ranging from energy storage to drug delivery.[1–6] The utility of MOFs mainly arises from their distinct three-dimensional topology that can be adjusted by varying either the metal cations or organic linking molecules. In particular, the porosity of this class of materials can be readily tuned,[7] which significantly affects their catalytic, energy storage, gas-separation, and dielectric properties. The nature of their porous three-dimensional framework results in peculiar elastic properties, which often lead to a significant mechanical destabilization as a function of minor external perturbations, such as pressure, temperature, or adsorption.[8–14] A detailed atomistic understanding of the interplay between intrinsic static structural features and lattice dynamical effects on the induced mechanical instability of MOFs is key to their effective design and use,[10,15] which is the aim of this study.

Zeolitic imidazolate frameworks (ZIFs) represent a class of MOFs comprised of tetrahedrally coordinated metal cations (often zinc or cobalt) with imidazolate-based organic linkers, which have recently attracted considerable attention.[16,17] One of the most widely studied ZIFs, ZIF-8, has been shown to exhibit a rich mechanochemical response as its sorption capacity increases with increasing pressure.[18–22] The origin of this peculiar feature is now understood in terms of a "gate-opening" or "swing-effect" sorption-induced structural change, where the imidazolate linkers rotate so as to increase the pore volume accessible to guest molecules.[19,23,24] When pressure is conveyed with a non-penetrating fluid (i.e. when no guest molecules are allowed in the pores), pristine ZIF-8 has been reported to undergo amorphization at 0.34 GPa where the porosity of its framework is retained but long-range order is disrupted.[25]

Little is known on the effect of pressure on the mechanical properties of ZIF-8. The anisotropic elastic response of ZIF-8 has been investigated at room temperature and ambient pressure via Brillouin scattering measurements, which provided elastic constants of C_{11}= 9.5 GPa, C_{12}= 6.9 GPa, and C_{44}= 0.97 GPa.[26] The corresponding isotropic adiabatic bulk modulus is $K_S = 7.7$ GPa. Single-crystal elastic constants have not yet been measured as a function of pressure, thus the evolution of the mechanical anisotropy of ZIF-8 as a function of pressure remains elusive. The only experimental evidence of the pressure dependence of the intrinsic mechanical properties of ZIF-8 is due to Chapman *et al.* who performed *in situ* X-ray diffraction measurements as a function of pressure.[25] When fitted to a third-order Birch-Murnaghan equation-of-state, the measured volume-pressure data, in the 0-0.34 GPa pressure range (i.e. before amorphization), provided a value of 6.5 GPa for the isothermal bulk modulus K_T (which is consistently lower than its adiabatic counterpart K_S), and a seemingly anomalous negative value for $K' = \partial K/\partial P$ of -4.6, which implies the decrease of the bulk modulus upon increasing pressure (i.e. mechanical softening

on pressure). From a theoretical point of view, classical molecular dynamics simulations were unable to confirm this peculiar feature as they described C_{11} and C_{12} elastic constants almost linearly increasing as a function of pressure in the whole 0-0.4 GPa pressure range thus implying a linearly increasing bulk modulus $K = 1/3(C_{11} + 2C_{12})$ and a positive K'.[12]

In this paper, we present the quantum-mechanical description of the evolution with pressure of the anisotropic mechanical properties of ZIF-8 and ZIF-67 (the spin-polarized isostructural analogue of ZIF-8 with Zn substituted by Co), along with an atomistic understanding of the corresponding structural changes and lattice vibrations. A peculiar non-linear trend of the anisotropic elastic response and mechanical stability of these ZIFs as a function of pressure is illustrated. In particular, three distinct pressure domains are identified according to the different anisotropic response of these materials (in terms of elastic moduli - Young's, bulk, shear – and velocities of propagation of directional elastic waves). The origin of the pressure-induced amorphization in ZIF-8 is confirmed to be related to its shear instability and it is shown to be due to asymmetric "gate-opening" and asymmetric "ring-breathing" structural changes; a similar amorphization in ZIF-67 is predicted. Furthermore, analysis of the lattice dynamics of the two ZIFs enables the partition of the nuclear-relaxation term of their directional elastic moduli into contributions from specific normal modes.

Quantum-mechanical calculations are performed with the CRYSTAL17 program.[27,28] The M06-2X hybrid exchange-correlation functional of the density functional theory (DFT) is used, which includes a fraction of exact non-local exchange of 54%. A split-valence double-ζ basis set is adopted. Convergence of the self-consistent-field process for the evaluation of energy and forces is set to 10^{-9} Ha. The fourth-rank elastic stiffness tensor is computed under different hydrostatic pressures by combining pressure-constrained structural relaxations and the evaluation of second energy density derivatives with respect to pairs of lattice deformations from two-sided numerical finite differences of analytical lattice forces computed at strained configurations with a strain amplitude of 1.5%.[29]

II. RESULTS AND DISCUSSION

As pressure increases, two main structural changes are induced in the pristine framework of the two ZIFs: i) the well-known "gate-opening" rotation of the imidazolate linkers, and ii) the rotation of the ZnN_4 (or CoN_4) tetrahedra. The former structural change has significant implications on the functionality of these materials and has been widely discussed.[18–21,23,24] The latter has generally been overlooked until it was recently shown to represent the intrinsic "order parameter" of the first-order phase transition occurring in ZIF-8 at high pressure.[30] The computed individual elastic constants of cubic ZIF-8 (C_{11}, C_{12} and C_{44}) are reported in Figure 1 as a function

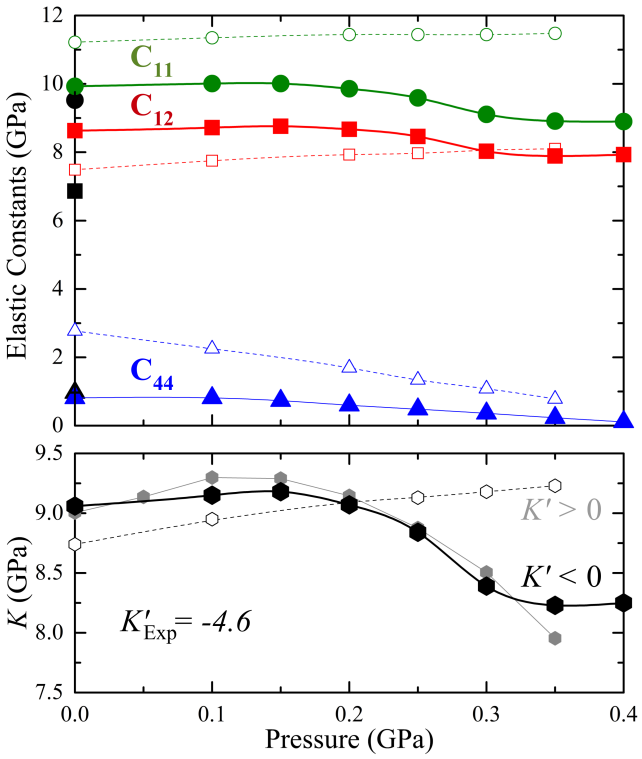

FIG. 1. (Upper panel) Elastic constants of ZIF-8 as a function of pressure (filled symbols, this study; empty symbols from Ref.[12]). Experimental values from Brillouin scattering at zero pressure are given as black symbols.[26] (Lower panel) Bulk modulus K as a function of pressure as determined from the computed elastic constants $K_{\rm elast}$ (black filled symbols) and from the pressure-volume equation-of-state $K_{\rm EoS}$ (grey filled symbols). Data from classical molecular dynamics simulations are reported as empty symbols[12]. From *in situ* X-ray diffraction, it is $K'_{\rm Exp}$ = -4.6.[25]

of pressure, in the 0-0.4 GPa range. At zero pressure, the agreement with the experimental values (black symbols) from room temperature Brillouin scattering measurements is rather satisfactory (the computed values being consistently higher because of neglected thermal effects). Notably, the agreement is very good for the shear C_{44} constant, whose low value of about 1 GPa makes it particularly critical to be accurately described. This confirms the high numerical precision of the simulations. Upon pressure, we find that both C_{11} and C_{12} (the two elastic moduli involved in the definition of the bulk modulus K) initially increase slightly up to $P = 0.15$ GPa and then decrease for $P > 0.2$ GPa. As pressure increases, the C_{44} elastic modulus is found to be almost constant up to $P = 0.1$ GPa and then to linearly decrease. Let us stress that this trend for the elastic constants is qualitatively different with respect to that reported in the only previous investigation on such properties from classical molecular dynamics simulations, particularly so for the C_{11} and C_{12} moduli (see thin dashed lines in Figure 1)[12]. The lower panel of Figure 1 shows the bulk mod-

ulus $K_{\rm elast} = 1/3(C_{11} + 2C_{12})$ as a function of pressure, as compared to the bulk modulus $K_{\rm EoS} = -V\partial P/\partial V$ derived from the pressure-volume equation-of-state. The two approaches are algorithmically and physically very different and yet provide a very consistent picture according to which the bulk modulus of ZIF-8 is initially increasing up to about $P = 0.15$ GPa and then decreases at $P > 0.2$ GPa. This means that as pressure increases ZIF-8 initially stiffens, followed by a mechanical softening at higher pressures (above 0.2 GPa). In the 0-0.35 GPa pressure range, this non-linear $K(P)$ trend corresponds to an average $K' = \partial K/\partial P$ of -3.8 (to be compared with the experimentally derived value of -4.6 by Chapman *et al.*[25]). We stress that with classical molecular dynamics simulations a positive K' was reported,[12] which confirms the need of accurate quantum-mechanical simulations for a reliable description of fine features such as the pressure dependence of the mechanical properties of ZIFs.

The evolution on pressure of the elastic anisotropy of ZIF-8 is illustrated in Figure 2 in terms of different indicators. The top panel reports 3D plots of the spatial dependence of the Young's modulus at pressures from 0 to 0.4 GPa (the axes are fixed for all pressures to aid in visualization). Three pressure domains can be clearly identified with distinct elastic features: i) at $P < 0.2$ GPa, ZIF-8 exhibits an anisotropic elastic response where the symmetry unique crystallographic directions of maximum mechanical stiffness and softness are ⟨111⟩ and ⟨100⟩, respectively ii) at $P = 0.2$ GPa, the system shows a perfectly isotropic elastic response, the spatial dependence of the Young's modulus being a sphere; iii) at $P > 0.2$ GPa, the mechanical response of ZIF-8 is again anisotropic, with a different (complementary) anisotropy with respect to the low-pressure regime: the crystallographic directions of maximum and minimum stiffness are now the ⟨100⟩ and ⟨111⟩, respectively. Overall, above 0.1 GPa of pressure, the Young's modulus of ZIF-8 shrinks as a function of pressure. Similar considerations can be made on the evolution on pressure of the shear modulus, see panel c) of Figure 2, where the spatial dependence of the maximum and minimum shear modulus is represented according to the conventions introduced in Ref. 31. The bottom panel of the figure reports polar plots of directional elastic wave velocities for ZIF-8 (i.e. the phase velocity at which an elastic wave propagates along different crystallographic directions with a longitudinal polarization). Directional elastic wave velocities are computed by solving Christoffel's equation[32,33] and further confirm the overall trend discussed above: at low pressures, elastic waves are propagating with the maximum velocity along the ⟨111⟩ directions, while at higher pressures the direction of maximum velocity switches to ⟨100⟩ (and symmetry-related ones).

A similar analysis has been performed for ZIF-67. At variance with ZIF-8, ZIF-67 is a spin-polarized system where each Co center hosts three unpaired electrons in its partially occupied d orbitals, and thus requires some special care in order to be accurately described.[34] Three distinct magnetic ordering configurations have been investigated: i) a symmetry-preserving ferromagnetic configuration where the unpaired electrons on all the Co centers in the primitive cell have spin-up; ii) a broken-symmetry half-antiferromagnetic configuration where the different Co centers in the primitive cell have spin-up and spin-down electrons; iii) a broken symmetry fully antiferromagnetic configuration where all adjacent Co centers exhibit alternating spin-up and spin-down couplings (this configuration required the use of the larger conventional cell to be modeled). The top panel of Figure 3 reports the spin density (i.e. difference between majority and

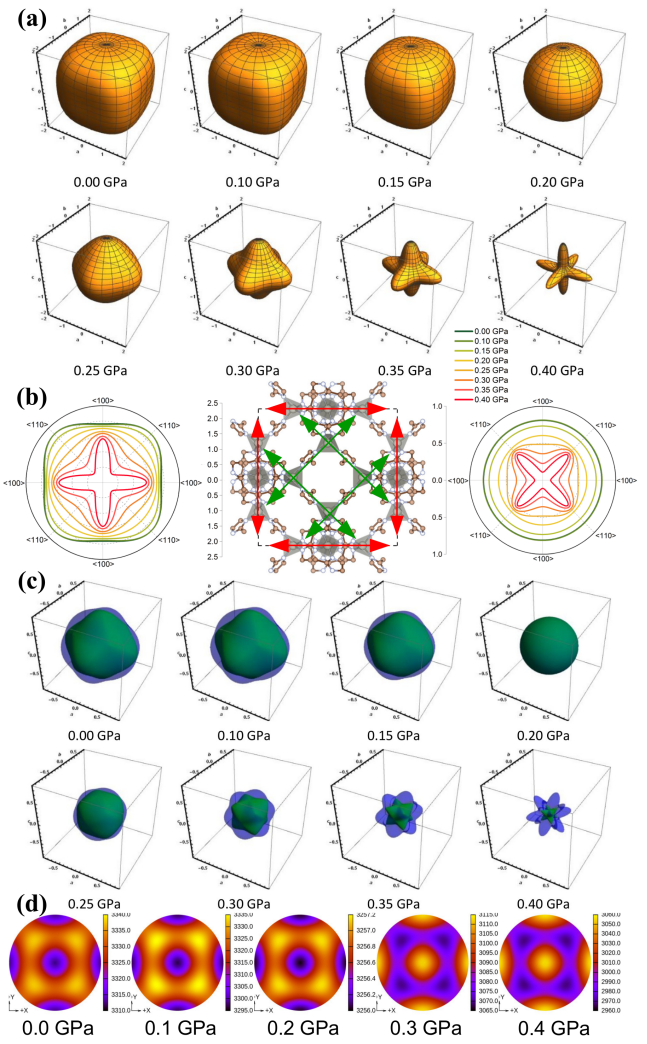

FIG. 2. Anisotropic mechanical properties of ZIF-8 as a function of pressure: (a) 3D representation of the Young's modulus (in GPa); (b) 2D representation in the xy plane of the Young's modulus (left), of the maximum shear modulus (right) and of the atomic structure of ZIF-8 (center); (c) 3D representation of the shear modulus - maximum and minimum values are shown as blue and green surfaces - (in GPa); (d) 2D polar representation of the longitudinal directional elastic wave velocities (in m/s).

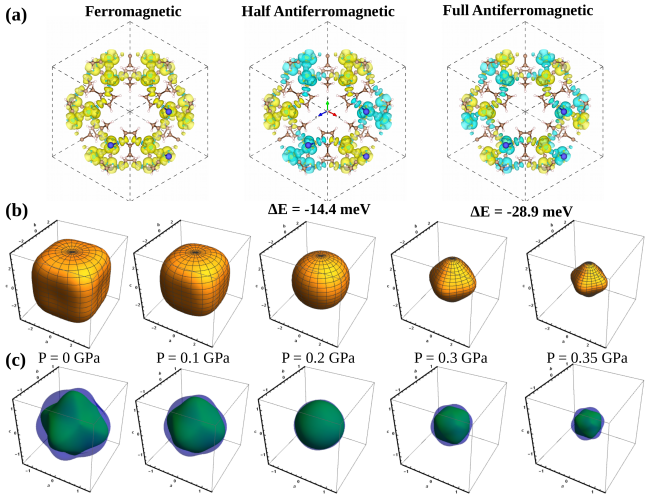

FIG. 3. (a) 3D spin density, $\rho^{\alpha} - \rho^{\beta}$, maps of ZIF-67 in different magnetic configurations; (b) 3D representation of the Young modulus (in GPa) as a function of pressure; (c) 3D representation of the shear modulus as a function of pressure - maximum and minimum values are shown as blue and green surfaces - (in GPa).

minority electron densities) of the three magnetic configurations. The broken-symmetry fully antiferromagnetic configuration is the most stable one (relative stabilities of different magnetic configurations are given in Figure 3). The overall mechanical behavior on compression of ZIF-67 is found to be very similar to that of ZIF-8, as can be seen from panels b) and c) of Figure 3, where the 3D representation of the Young's and shear elastic moduli is reported as a function of pressure. Also ZIF-67 has an initial anisotropy that progressively disappears up to $P = 0.2$ GPa, where it exhibits a perfectly isotropic mechanical response. As pressure is further increased, a different anisotropy is produced, which matches that observed in ZIF-8.

Pressure-induced amorphization is a common phenomenon in zeolites,[35,36] where the explicit link between mechanical destabilization and specific nuclear vibrations has been investigated and established.[37] Many ZIFs are also known to undergo a crystal-to-amorphous transition at relatively low pressures.[38–40] In particular, the mechanism of amorphization of ZIF-8 has already been unveiled by Ortiz *et al.*, who traced it back to the softening of the C_{44} shear elastic modulus as a function of pressure.[12] Indeed, from Figure 1, C_{44} is seen to linearly decrease with pressure, and to eventually violate the following Born condition for mechanical stability of cubic lattices under hydrostatic pressure:

$$C_{44} > P \, .$$

At a pressure of 0.35 GPa the condition above is no longer satisfied and the system becomes mechanically unstable to shear deformations. Amorphization of pristine ZIF-8 was experimentally reported to occur at 0.34 GPa,[25] again in remarkable agreement with our data. Analogously, we observe that ZIF-67 becomes mechanically unstable to shear deformations at a slightly higher pressure of 0.4 GPa, which would again most likely lead to amorphization.

In this study, we want to further analyze the amorphization mechanism of ZIFs by determining what kind of atomic structural changes are responsible for the shear softening of their framework. We start by recalling that elastic stiffness constants can always be decomposed into a purely electronic "clamped-nuclei" term and into a nuclear "internal-strain" term due to nuclear dynamics upon strain: $C_{vw}^{\rm tot} = C_{vw}^{\rm ele} + C_{vw}^{\rm nuc}$.[41,42] The nuclear term is by far the most computationally expensive and can be evaluated by relaxing atomic positions at strained lattice configurations or by computing the internal-strain and atomic Hessian tensors.[43–45] In Table S1 of the ESI,[46] we decouple electronic and nuclear contributions to the total elastic stiffness constants of ZIF-8 as a function of pressure. The following considerations can be made: i) the electronic contribution to the elastic constants is always large and positive; ii) the nuclear contribution is always large and negative so that the small total values of the elastic stiffness constants of ZIF-8 are due to the balance of the two contributions; iii) the electronic term is increasing upon pressure while the nuclear term is decreasing upon pressure. This means that the shear softening of ZIF-8 (as well as the decrease of its bulk modulus) as a function of pressure, eventually leading to amorphization, are due to internal-strain nuclear effects.

In order to gain further insight on the amorphization mechanism, the nuclear relaxation term can be partitioned into vibrational normal mode contributions. Formally, the total elastic constants of a crystal can be expressed as:[43–45]

$$C_{vw}^{\rm tot} = \frac{1}{V} \left. \frac{\partial^2 E}{\partial \eta_v \partial \eta_w} \right|_u - \frac{1}{V} \sum_{ai} \Lambda_{ai,v} \Gamma_{ai,w} \, , \qquad (1)$$

where the two terms on the right hand side are the electronic and nuclear contributions, respectively. Here, V is the cell volume, $\boldsymbol{\eta}$ is the pure strain tensor, and $\boldsymbol{\Lambda}$ and $\boldsymbol{\Gamma}$ are the force-response and displacement-response internal-strain tensors, respectively:

$$\Lambda_{ai,v} = \frac{\partial^2 E}{\partial u_{ai} \partial \eta_v} \quad \text{and} \quad \Gamma_{ai,v} = \sum_{bj} (H^{-1})_{ai,bj} \Lambda_{bj,v} \qquad (2)$$

where u_{ai} are Cartesian components of the displacement vector $\mathbf{u}_a$ of atom a (i=x, y, z), and where $\mathbf{H}$ is the interatomic force-constant Hessian matrix of energy second derivatives with respect to pairs of atomic displacements. When mass-weighted and diagonalized, $\mathbf{H}$ provides Brillouin zone-center phonon modes and corresponding vibration frequencies ω_p (being $p = 1, \ldots, 3N-3$ a phonon mode label, with N number of atoms per cell). This procedure allows for a physically meaningful partition of the nuclear relaxation contribution of Eq. (1) in terms of

phonon normal modes:

$$C_{vw}^{\mathrm{nuc}} = -\frac{1}{V}\sum_{p}\frac{\tilde{\Lambda}_{pv}\tilde{\Lambda}_{pw}}{\omega_p^2}\ , \tag{3}$$

where $\tilde{\mathbf{\Lambda}}$ is the mass-weighted internal-strain tensor: $\tilde{\Lambda}_{ai,v} = \Lambda_{ai,v}/\sqrt{M_a}$.

TABLE I. Harmonic normal mode contributions to the elastic moduli of ZIF-8. The lattice vibrations with the largest contributions to the elastic moduli of ZIF-8 are listed with their computed harmonic frequency ω, a label to identify them in the infrared and Raman spectra reported in Figure S1 of the ESI, the information on whether they are infrared and Raman active, and a brief description of the vibration mode. Their contribution C_ω to the elastic moduli is given in %.

Frequency ω	Label	IR	Raman	C_ω	Description
			C_{11} and C_{12}		
40 cm^{-1}	R1	no	yes	24%	Symmetric "gate-opening"
66 cm^{-1}	R2	no	yes	31%	Symmetric "gate-opening" (+ methyl rotation)
94 cm^{-1}	R3	no	yes	10%	Symmetric "gate-opening" (+ N–Zn–N bending)
			C_{44}		
52 cm^{-1}	I1	yes	yes	16%	Asymmetric breathing of the squared ring
63 cm^{-1}	I2	yes	yes	9%	Asymmetric "gate-opening"
127 cm^{-1}	I3	yes	yes	20%	Asymmetric "gate-opening" (+ methyl rotation)

We have computed the harmonic lattice dynamics of ZIF-8 (animations of all vibrational normal modes are available on-line through a link given in the ESI), applied the approach described above and observed that: i) all major contributions to the elastic moduli of ZIF-8 come from low-frequency (in the THz domain) collective vibrations, mostly involving motion of the imidazolate linkers; ii) the C_{11} and C_{12} elastic constants (and thus the bulk modulus) are predominantly affected by lattice vibrations involving the *symmetric* "gate-opening" motion (as such or as hybridized by the methyl rotation and N–Zn–N bending), where the four imidazolate linkers of the same squared channel swing perfectly in-phase (these vibrations are Raman active but infrared inactive); iii) the C_{44} elastic constant (and thus the pressure-induced shear instability) is related to the *asymmetric* "gate-opening" motion, where the two pairs of imidazolate linkers on the same squared channel swing out-of-phase and to the *asymmetric* "ring-breathing" motion of the four-membered ring (these vibrations are both infrared and Raman active). The lattice vibrations showing the largest contributions to the elastic constants of ZIF-8 are listed and described in Table I. Furthermore, it can be noted that most of the vibration modes related to the mechanical response of the system correspond to intense spectral features in either its Raman or infrared spectrum. Computed spectra of ZIF-8 are reported in the ESI where they are compared to the experimentally measured ones.

ACKNOWLEDGEMENTS

A.E. and J.M. thank the University of Torino and the Compagnia di San Paolo for funding (CSTO169372). M.R.R. acknowledges the Neutron Sciences Directorate at Oak Ridge National Laboratory (ORNL), managed by UT-Battelle, LLC, for the U.S. Department of Energy for a Clifford G. Shull Fellowship the National Energy Research Scientific Computing Center (NERSC), a U.S. Department of Energy Office of Science User Facility operated under Contract No. DE-AC02-05CH11231 for computing resources. M.T.R. thanks the University of Vermont for its continued support.

* alessandro.erba@unito.it

[1] J. A. Mason, J. Oktawiec, M. K. Taylor, M. R. Hudson, J. Rodriguez, J. E. Bachman, M. I. Gonzalez, A. Cervellino, A. Guagliardi, C. M. Brown, P. L. Llewellyn, N. Masciocchi, and J. R. Long, Nature Commun. **527**, 357 (2015).

[2] T. Tian, Z. Zeng, D. Vulpe, M. E. Casco, G. Divitini, P. a. Midgley, J. Silvestre-albero, J.-c. Tan, P. Z. Moghadam, and D. Fairen-Jimenez, Nat. Mater. **17**, 174 (2018).

[3] J. Zhuang, C.-H. Kuo, L.-Y. Chou, D.-Y. Liu, E. Weerapana, and C.-K. Tsung, ACS Nano **8**, 2812 (2014).

[4] M. R. Ryder and J.-C. Tan, Materials Science and Technology **30**, 1598 (2014).

[5] P. Horcajada, T. Chalati, C. Serre, B. Gillet, C. Sebrie, T. Baati, J. F. Eubank, D. Heurtaux, P. Clayette, C. Kreuz, J.-s. Chang, Y. K. Hwang, V. Marsaud, P.-n. Bories, L. Cynober, S. Gil, G. Férey, P. Couvreur, and R. Gref, Nat. Mater. **9**, 172 (2009).

[6] M. Vallet-regí, F. Balas, and D. Arcos, Angew. Chem. Int. Ed. **46**, 7548 (2007).

[7] B. Teng, R. Hao, M. Shengqian, C. Dapeng, L. Jianhui, J. Xiaofei, W. Wenchuan, X. Jun, D. Feng, S. Jason, Q. Shilun, and Z. Guangshan, Angewandte Chemie **121**, 9621 (2009).

[8] T. D. Bennett, J. Sotelo, J.-C. Tan, and S. A. Moggach, CrystEngComm **17**, 286 (2015).

[9] M. R. Ryder, T. D. Bennett, C. S. Kelley, M. D. Frogley, G. Cinque, and J.-C. Tan, Chem. Commun. **53**, 7041 (2017).

[10] M. R. Ryder, B. Civalleri, G. Cinque, and J.-C. Tan, CrystEngComm **18**, 4303 (2016).

[11] M. E. Casco, J. Fernandez-Catala, M. Martinez-Escandell, F. Rodriguez-Reinoso, E. V. Ramos-Fernandez, and J. Silvestre-Albero, Chem. Commun. **51**, 14191 (2015).

[12] A. U. Ortiz, A. Boutin, A. H. Fuchs, and F.-x. Coudert, J. Phys. Chem. Lett. **4**, 1861 (2013).

[13] M. R. Ryder and J.-C. Tan, Dalton Trans. **45**, 4154 (2016).

[14] M. R. Ryder, B. Civalleri, and J.-C. Tan, Phys. Chem. Chem. Phys. **18**, 9079 (2016).

[15] M. R. Ryder, B. Van de Voorde, B. Civalleri, T. D. Bennett, S. Mukhopadhyay, G. Cinque, F. Fernandez-Alonso, D. De Vos, S. Rudić, and J.-C. Tan, Phys. Rev. Lett. **118**, 255502 (2017).

[16] G. Lu and J. T. Hupp, J. Am. Chem. Soc. **132**, 7832 (2010).

[17] Y. Tingxu, S. G. Min, and C. T. Shung, Advanced Energy Materials **2**, 1358.

[18] S. A. Moggach, T. D. Bennett, and A. K. Cheetham, Angew. Chem. Int. Ed. **48**, 7087 (2009).

[19] D. Fairen-Jimenez, S. A. Moggach, M. T. Wharmby, P. A. Wright, S. Parsons, and T. Duren, J. Am. Chem. Soc. **133**, 8900 (2011).

[20] L. Zhang, Z. Hu, and J. Jiang, J. Am. Chem. Soc. **135**, 3722 (2013).

[21] J. Im, N. Yim, J. Kim, T. Vogt, and Y. Lee, J. Am. Chem. Soc. **138**, 11477 (2016).

[22] D. Radhakrishnan and C. Narayana, J. Chem. Phys. **144**, 134704 (2016).

[23] M. E. Casco, Y. Q. Cheng, L. L. Daemen, D. Fairen-Jimenez, E. V. Ramos-fernandez, a. J. Ramirez-cuesta, and J. Silvestre-albero, Chem. Commun. **52**, 3639 (2016).

[24] M. R. Ryder, B. Civalleri, T. D. Bennett, S. Henke, S. Rudić, G. Cinque, F. Fernandez-alonso, and J.-C. Tan, Phys. Rev. Lett. **113**, 215502 (2014).

[25] K. W. Chapman, G. J. Halder, and P. J. Chupas, J. Am. Chem. Soc. **131**, 17546 (2009).

[26] J.-C. Tan, B. Civalleri, C.-C. Lin, L. Valenzano, R. Galvelis, P.-F. Chen, T. D. Bennett, C. Mellot-Draznieks, C. M. Zicovich-Wilson, and A. K. Cheetham, Phys. Rev. Lett. **108**, 095502 (2012).

[27] R. Dovesi, A. Erba, R. Orlando, C. M. Zicovich-Wilson, B. Civalleri, L. Maschio, M. Rérat, S. Casassa, J. Baima, S. Salustro, and B. Kirtman, WIREs Comput. Mol. Sci. **8**, e1360 (2018).

[28] A. Erba, J. Baima, I. Bush, R. Orlando, and R. Dovesi, J. Chem. Theory Comput. **13**, 5019 (2017).

[29] A. Erba, A. Mahmoud, D. Belmonte, and R. Dovesi, J. Chem. Phys. **140**, 124703 (2014).

[30] W. Zhang, J. Maul, D. Vulpe, P. Z. Moghadam, D. Fairen-Jimenez, D. M. Mittleman, J. A. Zeitler, A. Erba, and M. T. Ruggiero, Science Advances (2018), submitted.

[31] A. Marmier, Z. A. Lethbridge, R. I. Walton, C. W. Smith, S. C. Parker, and K. E. Evans, Comput. Phys. Commun. **181**, 2102 (2010).

[32] M. J. P. Musgrave, *Crystal Acoustics* (Holden-Day, San Francisco, California, 1970).

[33] D. Muñoz-Santiburcio, A. Hernández-Laguna, and J. I. Soto, Comput. Phys. Commun. **192**, 272 (2015).

[34] K. E. El-Kelany, C. Ravoux, J. K. Desmarais, P. Cortona, Y. Pan, J. S. Tse, and A. Erba, Phys. Rev. B **97**, 245118 (2018).

[35] G. N. Greaves, F. Meneau, A. Sapelkin, L. M. Colyer, I. Gwynn, S. Wade, and G. Sankar, Nat. Mater. **2**, 622 (2003).

[36] N. Greaves and F. Meneau, J. Phys.: Condens Matter **16**, S3459 (2004).

[37] G. N. Greaves, F. Meneau, O. Majérus, D. G. Jones, and J. Taylor, Science **308**, 1299 (2005).

[38] T. D. Bennett, P. Simoncic, S. A. Moggach, F. Gozzo, P. Macchi, D. A. Keen, J.-C. Tan, and A. K. Cheetham, Chem. Commun. **47**, 7983 (2011).

[39] B. T. D., S. P. J., K. D. A., T. Jin-Chong, and C. A. K., Chemistry - A European Journal **19**, 7049 (2013).

[40] L. Bouessel du Bourg, A. U. Ortiz, A. Boutin, and F.-X. Coudert, APL Materials **2**, 124110 (2014).

[41] G. Saghi-Szabo, R. E. Cohen, and H. Krakauer, Phys. Rev. Lett. **80**, 4321 (1998).

[42] A. Dal Corso, M. Posternak, R. Resta, and A. Baldereschi, Phys. Rev. B **50**, 10715 (1994).

[43] A. Erba, D. Caglioti, C. M. Zicovich-Wilson, and R. Dovesi, J. Comput. Chem. **38**, 257 (2017).

[44] A. Erba, Phys. Chem. Chem. Phys. **18**, 13984 (2016).

[45] X. Wu, D. Vanderbilt, and D. R. Hamann, Phys. Rev. B **72**, 035105 (2005).

[46] See Supplemental Material at [URL] for electronic and nuclear contributions to the elastic constants of ZIF-8, for animations of normal modes of vibration of ZIF-8 and for low-frequency infrared and Raman spectra of ZIF-8.